Int. J. Adv. Appl. Math. and Mech. 2(3) (2015) 211 - 224 (ISSN: 2347-2529)
Journal homepage: www.ijaamm.com

IJAAMM

International Journal of Advances in Applied Mathematics and Mechanics

Mathematical analysis of pulsatile blood flow and heat transfer in oscillatory porous arteries

Research Article

A. Sinha *, A. Mondal

Department of Mathematics, Jadavpur University, R. S. C. Mullick Road, 700032, Kolkata, India

Received 29 January 2015; accepted (in revised version) 09 March 2015

Abstract: The present study aims to identify flow characteristics and heat transfer due to the body acceleration for blood through an porous artery exposed to a vibration environment. Blood flow is considered here to be governed by the equation of a Newtonian fluid model. Oscillatory flow in a porous channel is considered in this study. It pertains to a situation when the flow takes place between two porous plates lying parallel. The fluid is considered to be injected on one plate with a constant velocity, while it is sucked off at other with the same velocity. The plates are considered to be oscillating with a given velocity in their own planes. The problem is solved numerically. The numerical results for the velocity, temperature, wall shear stress and Nusselt number for the various values of the parameters involved are presented graphically and in tabular form. The study reveals that the flow is appreciably influenced by the presence of a magnetic field and also body acceleration.

MSC: 92B05 • 35Q79

Keywords: Pulsatile flow • Oscillating channel • Magnetic field • Body acceleration

1. Introduction

It is common knowledge that blood represents a concentrated dispersion formed by erythrocytes, leucocytes and thrombocytes in the plasma. The latter in turn is a colloidal solution of proteins having different molecular weights. The constituent components of blood are dominated by erythrocytes. In the free state, they have the shape of biconcave disks and they amount to approximately 93% of the total number of the elements and to 40-45% of the blood volume. Since erythrocytes have small negative charge, an applied magnetic field bears the capacity to influence the movement of erythrocytes and thereby to affect the flow of blood. Information available in the literatures regarding the exact mechanism by which the rheological properties of blood are effected by a magnetic field, is inadequate.

Higashi and his associates [11] and Yamagishi [1] investigated the orientation of erythrocytes in magnetic fields of strengths $8T$ and $4T$ respectively. They proclaimed that the erythrocytes orient themselves with their flat side in the direction of magnetic field. P.S.Rao and J.A.Rao [12] have numerically studied blood flow through an artery under the action of external magnetic field. Vardanyan [2] explored the potential use of MHD principles in prevention and rational therapy of arterial hypertension. From these discussions, it turns out that the hydrodynamic changes in the flow of blood can take place due to the external factors. It is known from the study of magnetohydrodynamics that when a transverse magnetic field is applied externally to a moving electrically conducting fluid, electric currents are induced in the fluid. The interaction between these induced currents and the applied magnetic field produces a body force (Lorentz force) which tends to retard the movement of fluid. Since

* Corresponding author.
E-mail address: aniruddha.sinha07@gmail.com

blood is an electrically conducting fluid, the motion of blood is expected to be controlled by applying magnetic field.

The phenomenon of vibration is usually conceived of as the oscillatory motion of the system. In the course of daily activities, the human body when subjected to a vibration environment, whole-body vibration can occur. It has been the observation of clinicians that vibration inhibits blood supply to different organs. They have observed that several health disorders originate from vibrating environments. In many cases, it can lead to grave consequences so far as our health is concerned. The effects of vibration become worse if the exposure to vibration takes place for a longer duration. There are experimental evidences that reveal that vibration energy can disrupt blood flow and effect the nerve system. Vibration can also disrupt the blood supply to the tissue around the spine, resulting in fatigue and inflammation.

The above description clearly indicate that vibration physiology has occupied the central place in Biomedical Engineering and Technology, as well as medical treatment.

Pulsatile flow of a fluid in a porous channel has been investigated by Wang [3], Bhatnagar [4], as well as Bhuyan and Hazarika [13] by considering the periodic pressure gradient. Ghosh [5] investigated the hydrodynamic fluctuating flow of a visco-elastic fluid in a porous channel where the channels oscillate with a given velocity in their own planes. In Cardiology, the study of the heart rate is studied by taking the ECG pattern in the presence of an external magnetic field that affects the blood flow. Ramachandra et al. [14] investigated the effect of a magnetic field on MHD oscillatory flow of blood oxygenation in a channel.

In recent time, a number of theoretical studies have been made to estimate the effects of body acceleration on the human circulatory system. Majhi and Nair [15] have studied an unsteady flow of third grade fluid under the influence of body acceleration. El-Shahed [6] studied the pulsatile flow of Newtonian fluid through a stenosed porous medium under the influence of periodic body acceleration. Chakravarty and Sanniggrahi [16] investigated theoretically the flow characteristics of blood through an artery subjected to whole-body acceleration. Sud et al. [17] discussed the flow characteristics of blood under the influence of externally applied periodic body acceleration in large and small arteries. Sud and Sekhon [18] analysed the blood flow through a model of human arterial system under periodic body acceleration. Keeping all these in mind, body acceleration has also been paid due attention in the present study. Alam [7] numerically studied an unsteady magnetodydrodynamic (MHD) free convective heat and mass transfer flow along an impulsively started infinite inclined porous plate.

Hyperthermia treatment has been demonstrated as effective during cancer therapy in recent years. Its objective is to raise the temperature of pathological tissues above cytotoxic temperature $(40-45^0\text{c})$ without overexposing healthy tissues [19]-[21]. Temperature distribution within tissues primarily depends on tissue thermal conductivity, the heating sources power deposition pattern characteristics and heat transfer resulting from blood flow [22]. Crezee and Lagendijk [23] conducted a numerical study on the impact of large vessels on the temperature ununiformity during hyperthermia treatment assuming steady-state condition. Several studies have also been conducted to analyse the effect of oscillatory flow on the velocity profile without examining its effect on heat transfer [8] and [9]. However, later studies, like the early work by Siegel and Perlmutter [24], addressed the dependence of heat transfer characteristic on pulsatile flow in a channel. Kim et al. [25] analysed numerically the heat transfer characteristics of fully developed pulsatile flow in a channel. Devi and Kumari [26] investigated the slip flow effects on unsteady hydro-magnetic flow over a stretching surface with thermal radiation heat transfer. They solved the problem by using Nachtsheim Swigert integration scheme along with Runge Kutta shooting method. Reddy [10] analysed the thermal radiation effect on a viscous incompressible unsteady chemically reacting and hydromagnetic fluid flow past an impulsively started vertical plate. Craciunescu and Clegg [27] studied numerically the effect of blood velocity pulsations on temperature distribution and heat transfer within rigid blood vessels.

The aim of this paper is to study the unsteady hydromagnetic flow as well as the associated problem heat transfer in the case of blood flow through an oscillatory porous artery under the influence of body acceleration. The problem is solved numerically by using finite difference method. Considering an illustrative example, numerical computation was performed in order to estimate the flow, temperature and wall shear stress for various values of Hartman number, Grashof number, Prandtl number and Eckert number. The study has the promise of significant applications in electromagnetic therapy, which has gained much popularity in recent times (cf. [28, 29]).

2. Mathematical modeling of the problem

Blood is treated here as a viscous incompressible electrically conducting fluid. We consider an unsteady hydromagnetic flow past infinite horizontal oscillatory porous plates under the influence of periodic body acceleration. A physical sketch of the geometry is shown in Fig. 1. In the Cartesian co-ordinate system x'-axis is assumed to be along the lower plate in the direction of the flow and y'-axis normal to it. The porous walls of the channel can be

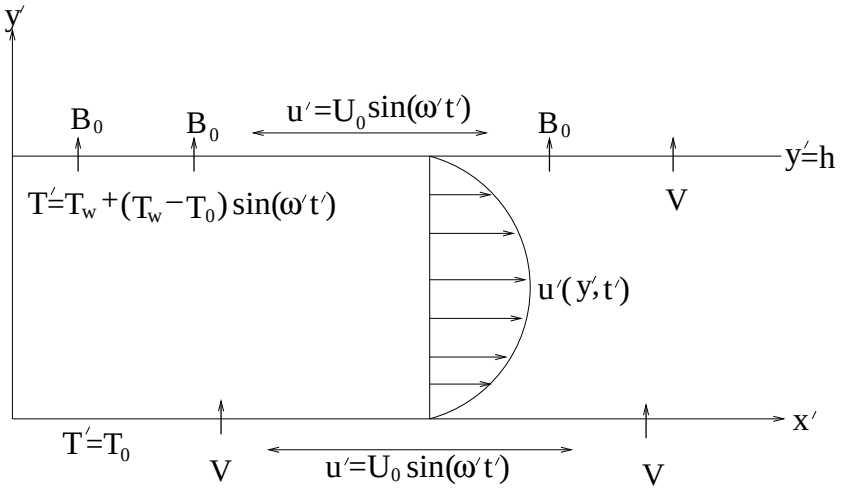

Fig. 1. Physical sketch of the problem

represented by $y' = 0$ and $y' = h$ (h being the channel-width). The fluid is injected by one plate with constant velocity V and sucked off by the other plate with the same velocity. A uniform magnetic field B_0 is applied normal to the direction of the flow. In this analysis, it is assumed that magnetic Reynolds number is much less than unity, so that the induced magnetic field is negligible in comparison to the applied magnetic field.
With all the above-mentioned consideration, the equations that govern the flow of fluid may be written as

$$\frac{\partial u'}{\partial x'} = 0 \tag{1}$$

$$\frac{\partial u'}{\partial t'} + V\frac{\partial u'}{\partial y'} = -\frac{1}{\rho}\frac{\partial p'}{\partial x'} + \nu\frac{\partial^2 u'}{\partial y'^2} + g\beta(T' - T_0) - \frac{\sigma B_0^2}{\rho}u' + G'(t') \tag{2}$$

$$0 = -\frac{1}{\rho}\frac{\partial p'}{\partial y'} \tag{3}$$

$$\frac{\partial T}{\partial t'} + V\frac{\partial T}{\partial y'} = \frac{k^\star}{\rho c_p}\frac{\partial^2 T}{\partial y'^2} + \frac{\sigma B_0^2}{\rho c_p}u'^2 \tag{4}$$

where u' represents axial velocity, V is the velocity of injection/suction, g is acceleration due to gravity, β is the coefficient of thermal expansion, B_0 being the applied magnetic field, p' and T' are the pressure and temperature, $G'(t')$ is periodic body acceleration, ν, σ and ρ are kinematic coefficient of viscosity, electrical conductivity and Density of blood, T_0 is the constant temperature of the lower plate, c_p and k* represent the specific heat at constant pressure and thermal conductivity. And the continuity Eq. (1) gives that u' is a function of y' and t' only.

When we exposed to a vibrating environment, the vibration of the platform will induce vibration in the arterial walls in the vicinity of the contact region and thereby the arterial wall have an oscillatory motion. This will, in turn, induce an oscillatory motion of blood that posses through the vibrating segment of the artery. In mathematical form, the corresponding boundary conditions can put as

$$u' = U_0'\sin(\omega' t'), \quad T' = 0 \quad at \quad y' = 0 \tag{5}$$

and

$$u' = U_0'\sin(\omega' t'), \quad T' = T_w + \sin(\omega' t')(T_w - T_0) \quad at \quad y' = h \tag{6}$$

where ω' denotes the heart pulse frequency.

For $t' > 0$, the flow is assumed to have a periodic body acceleration $G'(t')$ appeared in Eq. (2) has the expression of the form

$$G'(t') = a_0'\cos(\omega_1' t' + \phi) \tag{7}$$

where a_0' denotes the amplitude of body acceleration, ω_1' the frequency of the body acceleration and ϕ the phase difference.

For our present study we consider the following form of pressure gradient

$$-\frac{\partial p'}{\partial x'} = A_0' + A_1' \cos(\omega' t') \tag{8}$$

where A_0' and A_1' stand for constant amplitude of pressure gradient and amplitude of the pulsatile component gives rise to systolic and diastolic pressure. Let us now introduce the following non-dimensional co-ordinates:

$$x = \frac{x'}{h}, \quad y = \frac{y'}{h}, \quad t = \frac{t'V}{h} \tag{9}$$

the non-dimensional variables:

$$u = \frac{u'}{V}, \quad T = \frac{T' - T_0}{T_w - T_0} \tag{10}$$

and the non-dimensional parameters:

$$\omega = \frac{\omega' h}{V}, \quad \omega_1 = \frac{\omega_1' h}{V}, \quad A_0 = \frac{h^2 A_0'}{\mu V}, \quad A_1 = \frac{h^2 A_1'}{\mu V}, \quad a_0 = \frac{a_0' h^2}{\nu V} \tag{11}$$

Substituting (7) - (11) into the Eqs. (2) and (4), we get the following set of equations

$$Re\left(\frac{\partial u}{\partial t} + \frac{\partial u}{\partial y}\right) = F(t) + G(t) + \frac{\partial^2 u}{\partial y^2} + Gr\,T - M^2 u \tag{12}$$

and

$$\frac{\partial T}{\partial t} + \frac{\partial T}{\partial y} = \frac{1}{Pr}\frac{\partial^2 T}{\partial y^2} + \frac{M^2 Ec}{Re} u^2 \tag{13}$$

where $F(t) = A_0 + A_1 \cos(\omega t)$ and $G(t) = a_0 \cos(\omega_1 t + \phi)$

The boundary conditions (5) and (6) give rise to

$$u = U_0 \sin(\omega t), \qquad T = 0 \qquad at \quad y = 0 \tag{14}$$

$$u = U_0 \sin(\omega t), \qquad T = 1 + \sin(\omega t) \qquad at \quad y = 1 \tag{15}$$

where

$$U_0 = \frac{U_0'}{V}.$$

The other non-dimensional parameters that appear in the transformed equation presented above, are defined as follows:

$Re = \frac{Vh}{\nu}$ is the Reynolds number, $M = \sqrt{\frac{\sigma}{\mu}} B_0 h$ is the Hartman number, $Gr = \frac{g\beta h^2}{V\nu}(T_w - T_0)$ is the Grashof number, $Pr = \frac{\rho c_p h V}{k^*}$ is the Prandtl number and $Ec = \frac{V^2}{c_p(T_w - T_0)}$ is the Eckert number.

3. Numerical method

Eqs. (12) and (13) subjected to the boundary conditions (14) and (15) are solved numerically using the finite difference technique. The central difference scheme is employed to discretize the derivatives with respect to y in Eqs. (12) and (13) as

$$\frac{\partial R}{\partial y} = \frac{R_{i+1} - R_{i-1}}{2dy} + O(dy^2) \tag{16}$$

and

$$\frac{\partial^2 R}{\partial y^2} = \frac{R_{i+1} - 2R_i + R_{i-1}}{dy^2} + O(dy^2) \tag{17}$$

where R stands for u and T.

The values of u and T at the mesh point y_i are denoted by u_i and T_i respectively and at the j th time step, the same variables are denoted by u_i^j and T_i^j

where

$$y_i = i\,dy, \qquad i = 1,2,.....m$$
$$t_j = j\,dt, \qquad j = 0,1,.....$$

Now applying Crank-Nicolson formula for the Eqs. (12) and (13), we have

$$A_1 u_{i-1}^{j+1} + B_1 u_i^{j+1} + C_1 u_{i+1}^{j+1} = D_{1i}^j \tag{18}$$

$$A_2 T_{i-1}^{j+1} + B_2 T_i^{j+1} + C_2 T_{i+1}^{j+1} = D_{2i}^j \tag{19}$$

where

$$A_1 = -r_1 - r_2, \quad B_1 = 1 + r_2, \quad C_1 = r_1 - r_2,$$
$$D_{1i}^j = u_i^j + \frac{dt}{Re}(F^j + G^j - M^2 u_i^j + Gr\,T_i^j),$$
$$A_2 = -Re(r_1 + \frac{1}{Pr} r_2), \quad B_2 = 1 + 2\frac{Re}{Pr}$$
$$r_2, \quad C_2 = Re(r_1 - \frac{1}{Pr} r_2),$$
$$D_{2i}^j = T_i^j + \frac{dt\,M^2 Ec}{Re}(u_i^{j+1})^2,$$
$$r_1 = \frac{dt}{2dy\,Re}, \quad r_2 = \frac{dt}{dy^2 Re},$$
$$F^j = A_0 + A_1\cos(\omega t_j) \quad and \quad G^j = a_0\cos(\omega_1 t_j + \phi)$$

where dy and dt are the mesh size along the space and time directions.
The system of linear Eqs. (18) and (19) are expressed as tri-diagonal system of equations which are solved by using Thomas algorithm.

For $j = 0$, the system of Eq. (18) may be written as

$$a_i u_{i-1}^1 + b_i u_i^1 + c_i u_{i+1}^1 = d_i^0 \qquad for \quad i = 1,2,....,m \tag{20}$$

where

$$a_i = A_1 \qquad \text{for} \quad i = 2,3,...,m$$
$$b_i = B_1 \qquad \text{for} \quad i = 1,2,...,m$$
$$c_i = C_1 \qquad \text{for} \quad i = 1,2,....,m-1$$
$$d_i^0 = D_{1i}^0 \qquad \text{for} \quad i = 2,3,....,m-1$$
$$a_1 = 0, \quad c_m = 0, \quad d_1^0 = D_{11}^0 - A_1 u_0^0, \quad d_m^0 = D_{1m}^0 - C_1 u_m^0.$$

Suppose

$$u_i^1 = p_i u_{i+1}^1 + q_i \qquad for \quad i = 1,2,....,m \tag{21}$$

and

$$u_{i-1}^1 = p_{i-1} u_i^1 + q_{i-1} \qquad for \quad i = 1,2,....,m \tag{22}$$

For $i = 1$, from the Eq. (20) we get

$$p_1 = -\frac{c_1}{b_1}, \quad q_1 = \frac{d_1^0}{b_1}$$

Now eliminating u_{i-1}^1 from the equation (20) we get

$$u_i^1 = -\frac{c_i}{b_i + a_i p_{i-1}} u_{i+1}^1 + \frac{d_i^0 - a_i q_{i-1}}{b_i + a_i p_{i-1}} \qquad for \quad i = 1, 2, ..., m \tag{23}$$

where

$$p_i = -\frac{c_i}{b_i + a_i p_{i-1}}, \qquad i = 1, 2, ..., m$$

$$q_i = \frac{d_i^0 - a_i q_{i-1}}{b_i + a_i p_{i-1}}, \qquad i = 1, 2, ..., m$$

Let us take

$$u_{m+1}^1 = 0 \tag{24}$$

Using (24), from (21) we get

$$u_m^1 = q_m \tag{25}$$

Now using

$$u_i^1 = p_i u_{i+1}^1 + q_i$$

we can compute u_i^1, for $i = m-1, m-2, ..., 3, 2, 1$ in succession.
The same procedure can be adopted for any other time t.
Similarly we can solve (19) for temperature.
In the next section, we present the computational results for the major physical quantities, viz. the wall shear stress (τ_w) and Nusselt number (Nu) defined respectively by

$$\tau_w = \left(\frac{\partial u}{\partial y}\right)_{y=0} \quad \text{and} \quad Nu = -\left(\frac{\partial T}{\partial y}\right)_{y=0}$$

4. Results and discussion

In order to investigate numerical solution of pulsatile flow and heat transfer of blood through an oscillatory porous artery under the influence of a periodic body acceleration as well as an external magnetic field, the numerical technique described above was employed to solve the equations (12) and (13), subjected to the appropriate boundary conditions (14) and (15).

In order to obtain an estimate of flow and temperature variables, we have taken $\rho = 1050 kg\,m^{-3}$ and $\mu = 3.2 \times 10^{-3} kg\,m^{-1}s^{-1}$. Moreover, various values of the physical parameters a_0, ω, ω_1, M, Gr,, Pr and Ec have been chosen over a range, which are listed in each caption of the figures.

Computational work has been performed with $dy = 0.025$ and $dt = 0.01$ with 201 grid points. The computed results have been presented in the Figs. 2 - 12.

Figs. 2 - 5 focus on the dimensionless axial velocity u for different values of Hartman number M, Grashof number Gr, amplitude of body acceleration a_0 and frequency of body acceleration ω_1.

From Fig. 2, we see that the axial velocity decreases with the increase in Hartman number M, in the case of cooling of the arterial wall i,e, when $Gr > 0$. This observation agrees with the theory, because with the increase in Hartman number M, Lorentz force increases. It is known that Lorentz force opposes the flow. Thus with the increase in the strength of magnetic field, flow of blood will be impeded. It is also noted from this figure that the point at which the axial velocity attains its maximum is shifted towards the lower wall as the intensity of the magnetic field increases. It is also seen that for large value of Hartman number (M), the flow shows a tendency to separate in the adjoining region of the upper wall; this tendency however, gradually disappears as the value of Hartman number decreases. One can have an idea of the velocity distribution for the both cooling of the wall ($Gr > 0$) and heating of the wall ($Gr < 0$) from Fig. 3. It is seen from this figure that in the case of cooling, axial velocity increases as Grashof number increases, while in the case of heating, axial velocity decreases with increasing Grashof number. In the case of

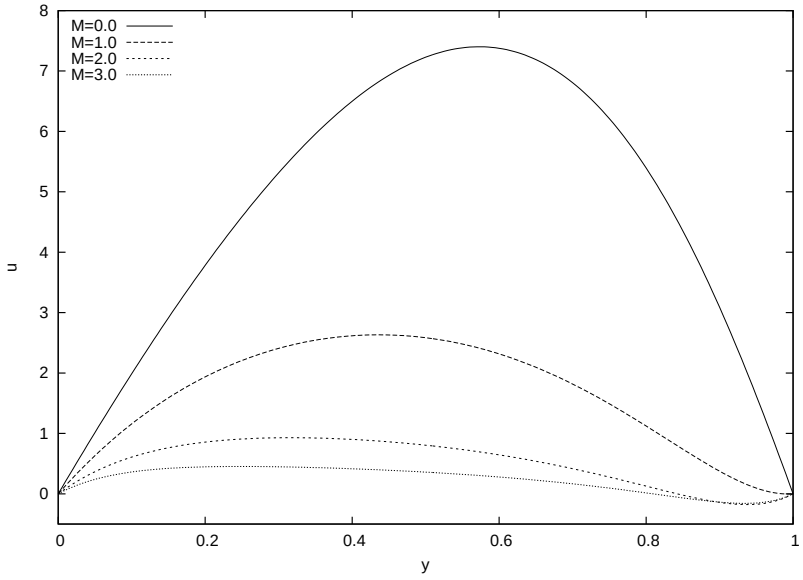

Fig. 2. Velocity distribution for different values of M^2 when $a_0 = 1.3$, $\omega_1 = 2.0$, $\omega = 2.0$, $Gr = 10.0$, $Pr = 0.71$, $Ec = 0.0002$ and $t = \frac{\pi}{2}$.

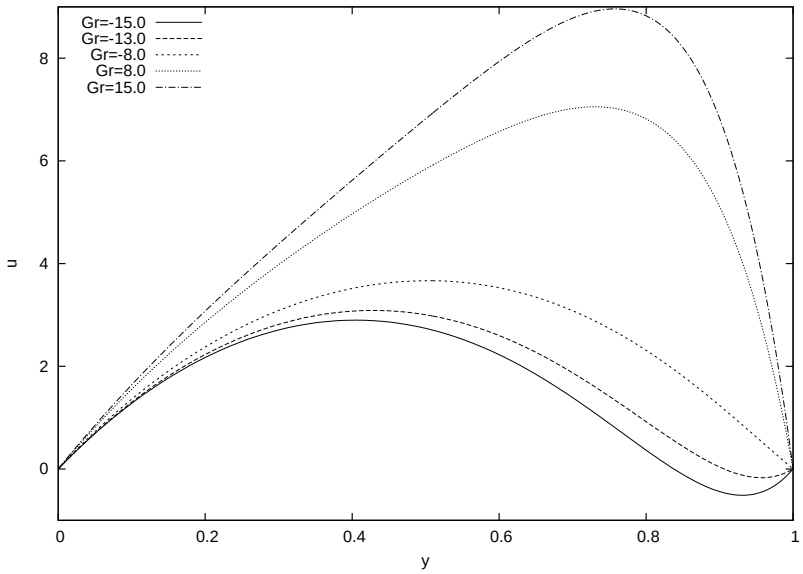

Fig. 3. Velocity distribution for different values of Gr when $a_0 = 1.3$, $\omega_1 = 2.0$, $\omega = 2.0$, $M = 0.8$, $Pr = 0.71$, $Ec = 0.0002$ and $t = \frac{\pi}{2}$.

heating, we also observe that for large values of Grashof number ($Gr = -13.0, -15.0$), the flow reversal can take place at some points between $y = 4.0$ and $y = 5.0$. In the same case, as Grashof number increases, the point at which velocity vanishes is shifted faraway the upper wall. This point is point of inflexion.

In the case of cooling of the arterial wall, the variation of the axial velocity for different amplitude of the body acceleration a_0 is shown in Fig. 4 when $\omega_1 t = 2\pi$ and $\phi = 0$. It reveals that the axial velocity increases as the amplitude of the body acceleration increases. This observation agrees with the fact that when $\omega_1 t = 2\pi$ and $\phi = 0$, the body acceleration $G(t)$ is positive and so as a_0 increases, $G(t)$ increases. It is known that body acceleration reduces the flow resistance and so the velocity of the blood flow increases with the increase in body acceleration.

Fig. 5 gives the distribution of axial velocity for different values of frequency of body acceleration ω_1 when $t = \frac{\pi}{2}$ and $\phi = 0$, in the case of cooling of the arterial wall. It is seen from this figure that the axial velocity decreases as ω_1 increases. As amplitude of body acceleration is positive, so for $0 \leq \omega_1 \leq 2$, the body acceleration $G(t)$ decreases as ω_1 increases. In the other words, flow resistance increases with the increase in frequency of body acceleration. So

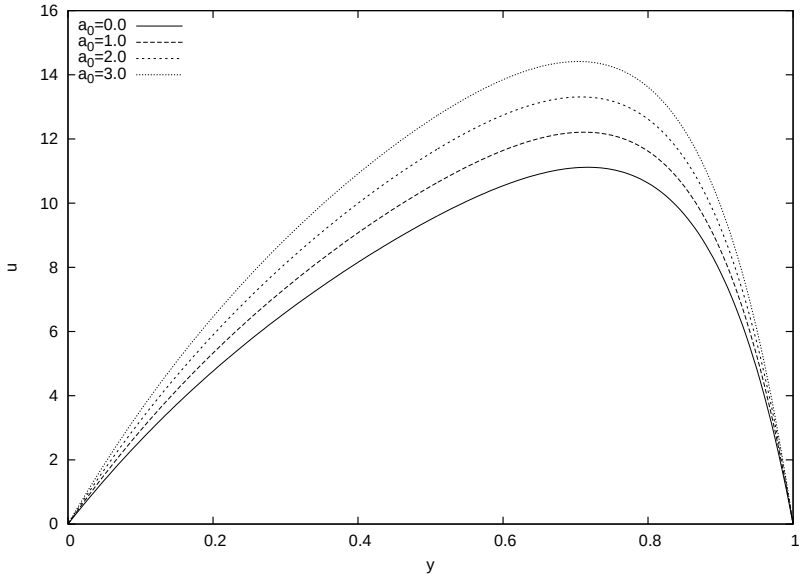

Fig. 4. Velocity distribution for different values of a_0 ($\omega = 2.0$, $\omega_1 = 2.0$, $M = 0.8$, $Gr = 10.0$, $Pr = 0.71$, $Ec = 0.0002$ and $t = \pi$

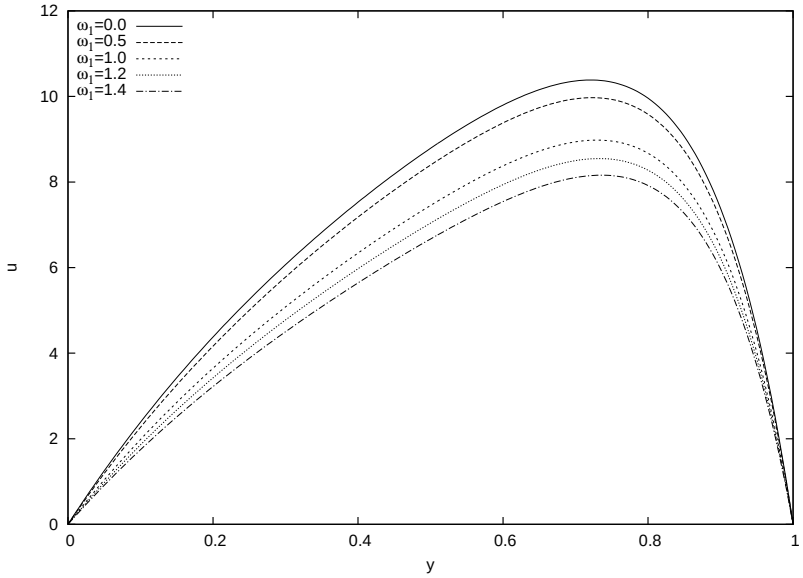

Fig. 5. Velocity for different values of ω_1 ($\omega = 2.0$, $a_0 = 1.3$, $M = 0.8$, $Gr = 10.0$, $Pr = 0.71$, $Ec = 0.0002$ and $t = \frac{\pi}{2}$).

the velocity of blood decreases with the increase in ω_1.
Fig. 6 exhibits the distribution of the axial velocity at different instants of time t when $\omega = \omega_1 = 1.0$ and $\phi = 0$. From this figure, it may be observed different features in different time intervals. In $0 \le t \le \frac{\pi}{4}$, axial velocity increases with time but in $\frac{\pi}{4} \le t \le \frac{\pi}{2}$, first axial velocity decreases upto a certain height of the artery and beyond which velocity increases, while in the whole time interval $\frac{\pi}{2} \le t \le \pi$, velocity decreases.

Figs. 7 - 8 give some characteristic temperature profile for different values of Prandtl number Pr and Eckert number Ec in the case of cooling of the wall. It may be observed from Fig. 7 that temperature decreases with increasing Prandtl number while Fig. 8 shows that temperature increases with increasing Eckert number.

Fig. 9 exhibits the temperature distribution at different instants of time when $\omega = \omega_1 = 2.0$ and $\phi = 0$. It is seen from this figure that in the time interval $\frac{\pi}{8} \le t \le \frac{\pi}{4}$, the temperature increases but in $\frac{\pi}{4} \le t \le \frac{\pi}{2}$, the temperature decreases.

Figs. 10 and 11 show the variation of wall shear stress which is an important factor in hemodynamics, with Hartman number M for different values of amplitude of body acceleration a_o and Grashof number Gr. Fig. 10 is plotted when $\omega = \omega_1 = 2.0$, $\phi = 0$, $t = \pi$ and $Gr = 10.0$. It is observed from this figure that wall shear stress increases

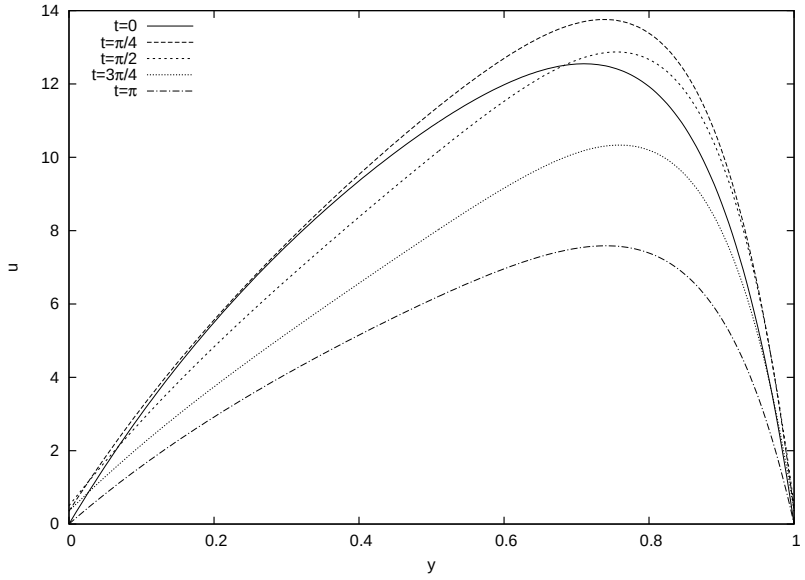

Fig. 6. Velocity field at different instants of time t when $\omega = 1.0$, $a_0 = 1.3$, $\omega_1 = 1.0$, $M = 0.8$, $Gr = 10.0$, $Pr = 0.71$ and $Ec = 0.0002$.

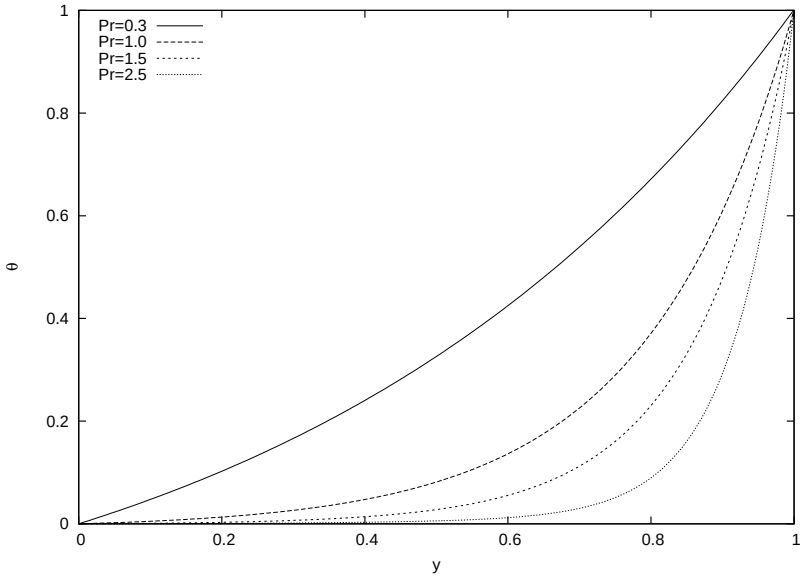

Fig. 7. Temperature distribution for different values of Pr ($a_0 = 1.3$, $\omega = 2.0$, $\omega_1 = 2.0$, $M = 0.8$, $Gr = 10.0$, $Ec = 0.0002$ and $t = \frac{\pi}{2}$).

with increasing the amplitude of the body acceleration. Fig. 11 shows that in the case of cooling, wall shear stress increases as Grashof number increases while a reverse trend is observed in the case of heating.

Fig. 12 presents the variation of wall shear stress with time for different values of a_0. It shows that amplitude of the oscillation of the wall shear stress increases with the increase of the amplitude of the body acceleration.
Table 1 gives the numerical values of heat transfer coefficient for different values of a_0, ω_1, M, Gr, Pr and Ec when $Re = 1.2$, $\omega = 1.0$ and $\phi = 0$ at time $t = \frac{\pi}{2}$. Table 1 shows that for increase in ω_1 and Pr heat transfer coefficient increases while increase in a_0 or M or Gr or Ec gives rise to reduction in heat transfer coefficient.

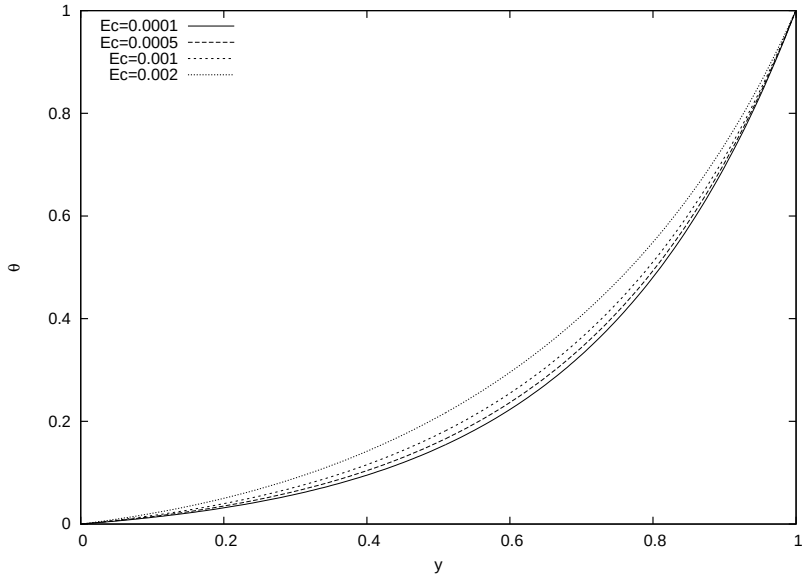

Fig. 8. Temperature distribution for different values of Ec ($a_0 = 1.3$, $\omega = 2.0$, $\omega_1 = 2.0$, $M = 0.8$, $Gr = 10.0$, $Pr = 0.71$ and $t = \frac{\pi}{2}$).

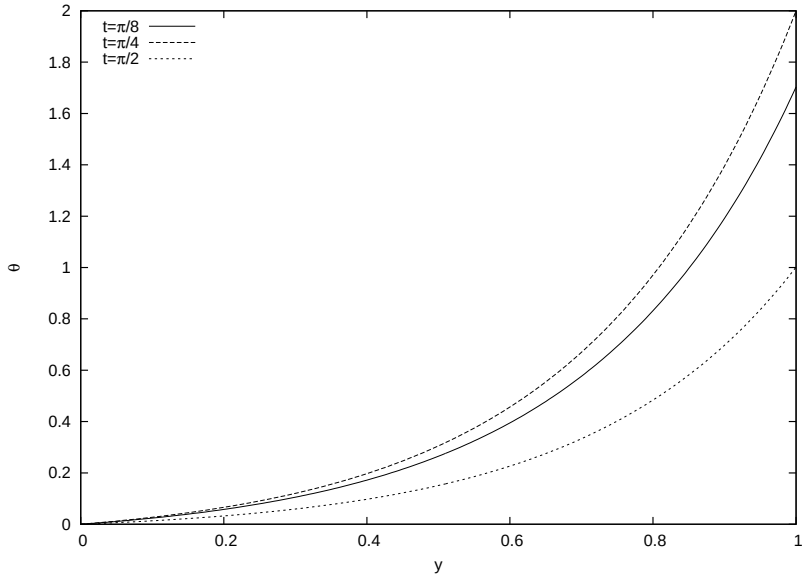

Fig. 9. Temperature field at different instants of time t ($\omega = 2.0$, $a_0 = 1.3$, $\omega_1 = 2.0$, $M = 0.8$, $Gr = 10.0$, $Pr = 0.71$ and $Ec = 0.0002$).

Table 1. Heat transfer coefficient (Nu) for cooling of the arterial wall

a_0	ω_1	M	Gr	Pr	Ec	Nu
1.0	0.5	1.5	5.0	0.8	0.0001	-0.03119472
2.0	0.5	1.5	5.0	0.8	0.0001	-0.03137328
1.0	1.2	1.5	5.0	0.8	0.0001	-0.03097949
1.0	0.5	2.5	5.0	0.8	0.0001	-0.03598482
1.0	0.5	1.5	10.0	0.8	0.0001	-0.03140222
1.0	0.5	1.5	5.0	1.4	0.0001	-0.00333186
1.0	0.5	1.5	5.0	0.8	0.0005	-0.03552763

5. Concluding remarks

- The motivation behind the study has been to make some theoretical predictions on the flow of blood in arteries, when there is an external agency that includes vibration in the human body and there by at least some of

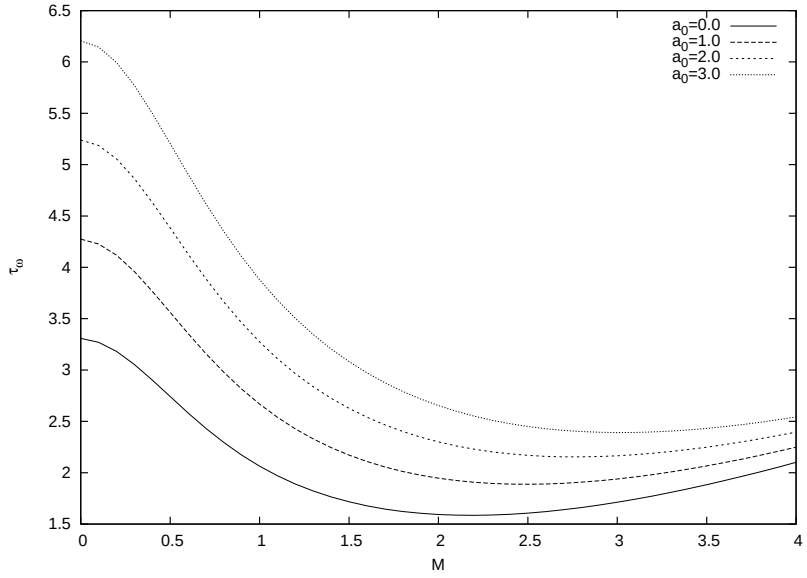

Fig. 10. Variation of wall shear stress τ_w with M for different values of a_0, with $\omega = 2.0$, $\omega_1 = 2.0$, $M = 0.8$, $Gr = 10.0$, $Pr = 0.71$, $Ec = 0.0002$ and $t = \frac{\pi}{2}$

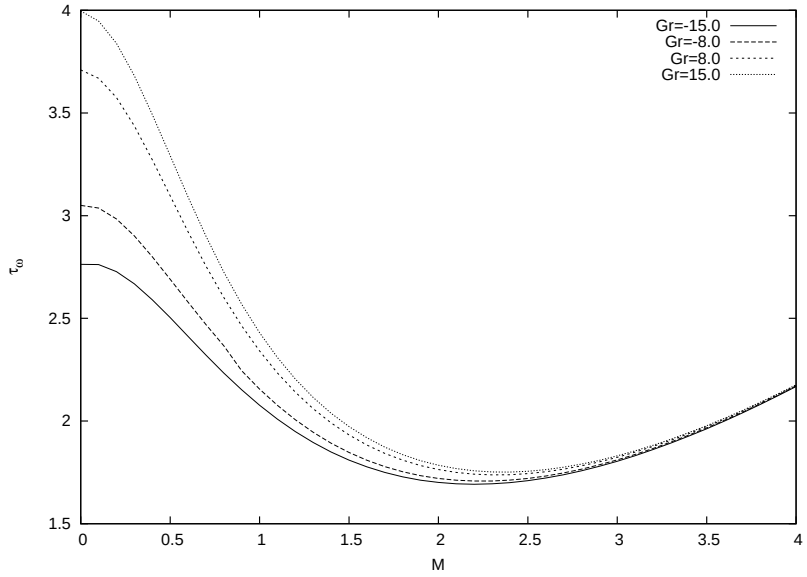

Fig. 11. Variation of wall shear stress τ_w with M for different values of Gr, with $\omega = 2.0$, $\omega_1 = 2.0$, $a_0 = 1.3$, $M = 0.8$, $Pr = 0.71$, $Ec = 0.0002$ and $t = \frac{\pi}{2}$.

arteries of the arterial tree get vibrated.

- The effect of body acceleration on flow and heat transfer of blood through an oscillatory porous artery has been studied. The artery is considered exposed to an external magnetic field. The wall oscillations are considered to induce oscillatory behaviour of the flow.
- The computational results reveal very clearly that both the velocity and temperature of the blood are affected to an appreciable extent to a vibration environment in the course of daily activities of life.
- The theoretical predictions of the study are believed to have useful applications in many engineering problems that involved heating and cooling. It also bears the potential to provide important applications in the study of various problems of dynamics of physiological fluids, like blood. Some of the results presented should have several clinical applications, for example, in reduction of blood flow by applying magnetic field during surgery.
- The result shows that in the case of cooling, the Nusselt number (Nu) increases from negative value with increase of the Prandtl number Pr, that is temperature gradient at the surface is decreasing from positive value.

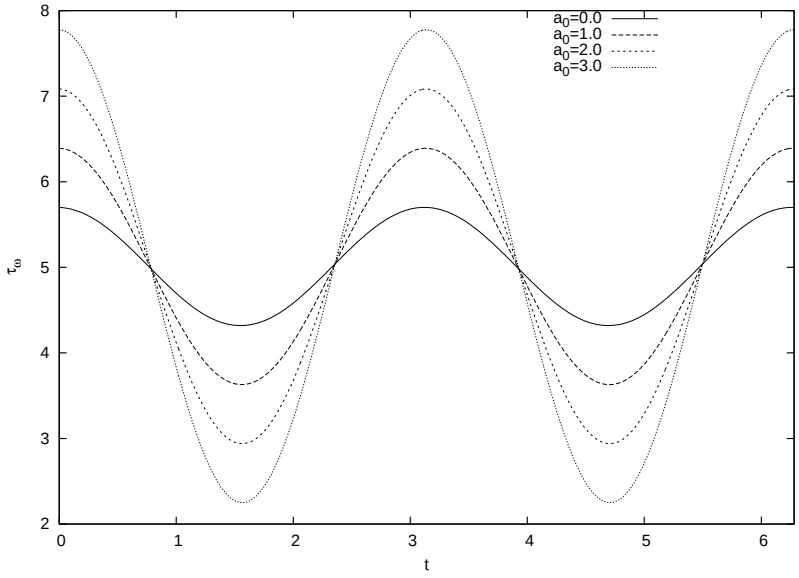

Fig. 12. Variation of wall shear stress τ_w with time for different values 0f a_0 when $\omega = 2.0$, $\omega_1 = 2.0$, $M = 0.8$, $Gr = 10.0$, $Pr = 0.71$ and $Ec = 0.0002$.

Which means that the blood is gaining temperature from the oscillatory arterial wall. So temperature of the blood can be controlled by increasing or decreasing the Prandtl number.

Acknowledgement

The first author is grateful to the SERB, DST, New Delhi for financial support in executing this work.

References

[1] A. Yamagishi, Biological systems in high magnetic field, J. Magn. Mater. 90 (1990) 43-46.
[2] V.A. Vardanyan, Effect of Magnetic field on Blood flow, Biofizika 18 (1973) 491-496.
[3] C.Y. Wang, Pulsatile flow in a porous channel, J. Appl. Mech. 38 (1971) 553-555.
[4] R.K. Bhatnagar, Fluctuating flow of a viscoelastic fluid in a porous channel, J. Appl. Mech. 46 (1979) 21-25.
[5] S.K. Ghosh, Hydromagnetic fluctuating flow of a viscoelastic fluid in a porous channel, J. Appl. Mech. 74 (2007) 177-180.
[6] M. El-Shahed, Pulsatile flow of blood through a stenosed porous medium under periodic body acceleration, Appl. Math. Comput. 138 (2003) 479-488.
[7] M.S. Alam, Transient thermophoretic particle deposition on MHD free convective and viscous dissipative flow along an inclined surface considering Dufour-Soret effects, Int. J. Adv. Appl. Math. and Mech. 1(3) (2014) 121-134.
[8] J.R. Womersley, Oscillatory motion of a viscous liquid in a thin walled elastic tube. I: The linear approximation for long waves, Philos. Mag. 46 (1955) 199-221.
[9] S. Uchida, The pulsating viscous flow superimposed on the steady laminar motion of incompressible fluid in a circular pipe, Z. Angew.Math. Phys. 7 (1956) 403-422.
[10] M.G. Reddy, Heat and mass transfer effects on unsteady MHD flow of a chemically reacting fluid past an impulsively started vertical plate with radiation, International Journal of Advances in Applied Mathematics and Mechanics 1 (2013) 1-15.
[11] A. Higashi, A. Yamagishi, T. Takeuchi, N. Kawaguchi, S. Sagawa, S. Onishi, M. Date, Orientation of erythrocytes in a strong static magnetic field, Blood 82 (1993) 1328-1334.
[12] P.S.Rao, J.A. Rao, Numerical solution of non-steady magnetohydrodynamic flow of blood through a porous channel, J. Biomed. Eng. 10 (1988) 293-295.
[13] B.C. Bhuyan, G.C. Hazarika, Effect of Magnetic field on Pulsatile flow of Blood in a Porous Channel, Bio-Science Research Bulletin 17 (2001) 105-112.
[14] A.R. Rao, K.S. Desikachar, MHD oscillatory flow of blood through channels of variable cross section, Int. J. Eng. Sci. 24 (1986) 1615-1628.

[15] S.N. Majhi, V.R. Nair, Pulsatile flow of third grade fluids under body acceleration modelling flow, Int. J. Eng. Sci. 32 (1994) 839-846.
[16] S. Chakravarty, A.K. Sannigrahi, A nonlinear mathematical model of blood flow in a constricted artery experiencing body acceleration, Math comput Model 29 (1999) 9-25.
[17] V.K. Sud, H.E.V. Gierke, I. Kaleps, H.L. Oestreicher, Blood flow under the influence of externally applied periodic body acceleration in large and small arteries, Med Biol Eng Comput. 21 (1983) 446-452.
[18] V.K. Sud, G.S. Sekhon, Analysis of blood flow through a model of human arterial system under periodic body acceleration, J. Biomech. 19 (1986) 929-941.
[19] J.R. Oleson, D.A. Sim, M.R. Manning, Analysis of prognostic variables in hyperthermia treatment of 161 patients, Int. J. Radiat. Oncol. Biol. Phys. 10 (1984) 2231-2239.
[20] S.B. Field, J.W. Hand, An Introduction to the Practical Aspects of Hyperthermia, Taylor & Francis, New York, 1990.
[21] M.W. Field, T.V. Dewhirst, Hyperthermia in the Treatment for Cancer, Upjohn, Kalamazoo, MI, 1988.
[22] S.H. Reinhold, B. Endrich, Tumor microcirculation as a target for hyperthermia, Int. J. Hyperther. 2 (1986) 111-137.
[23] J. Crezee, J.W. Lagendijk, Temperature uniformity during hyperthermia: the impact of large vessels, Phys. Med. Biol. 37 (1992) 1321-1337.
[24] R. Siegel, M. Perlmutter, Heat transfer for pulsating laminar duct flow, ASME J. Heat Transfer 8 (1962) 111-116.
[25] S.Y. Kim, B.H. Kang, J.M. Hyun, Heat transfer in the thermally developing region of a pulsating channel flow, Int. J. Heat Mass Transfer 36 (1993) 4257-4266.
[26] S.P.A. Devi, D.V. Kumari, Numerical investigation of slip flow effects on unsteady hydromagnetic flow over a stretching surface with thermal radiation, Int. J. Adv. Appl. Math. and Mech. 1(4) (2014) 20-32.
[27] O.I. Craciunescu, C.T. Clegg, Pulsatile blood flow effects on temperature distribution and heat transfer in rigid vessels, ASME J. Biomech. Eng. 123 (2001) 500-505.
[28] J.C. Misra, A. Sinha, G.C. Shit, Flow of a biomagnetic viscoelastic fluid: application to estimation of blood flow in arteries during electromagnetic hyperthermia, a therapeutic procedure for cancer treatment, Applied Mathematics and Mechanics (English Edition) 31 (2010) 1405-1420.
[29] A. Miaskowski, A. Krawczyk, Y. Ishihara, Computer modelling of magnetotherapy in orthopedic treatments, Computer modelling of magnetotherapy 29 (2010) 1015-1021.

Appendix

$$Re\left(\frac{\partial u}{\partial t}+\frac{\partial u}{\partial y}\right)=F(t)+G(t)+\frac{\partial^2 u}{\partial y^2}+GrT-M^2u$$

$$Re\left[\frac{u_i^{j+1}-u_i^{j+1}}{dt}+\frac{u_{i+1}^{j+1}-u_{i-1}^{j+1}}{2dy}\right]=F^j+G^j+\frac{u_{i+1}^{j+1}-2u_i^{j+1}+u_{i-1}^{j+1}}{dy^2}-M^2u_i^j+GrT_i^j$$

$$\left(-\frac{dt}{2Redy}-\frac{dt}{Redy^2}\right)u_{i-1}^{j+1}+\left(1+\frac{2dt}{Redy^2}\right)u_i^{j+1}+\left(\frac{dt}{2Redy}-\frac{dt}{Redy^2}\right)u_{i+1}^{j+1}=u_i^j+\frac{dt}{Re}\left(F^j+G^j-M^2u_i^j+GrT_i^j\right)$$

$$A_1u_{i-1}^{j+1}+B_1u_i^{j+1}+C_1u_{i+1}^{j+1}=D_{1i}^j$$

where

$$A_1=-r_1-r_2,\quad B_1=1+r_2,\quad C_1=r_1-r_2,$$

$$D_{1i}^j=u_i^j+\frac{dt}{Re}(F^j+G^j-M^2u_i^j+GrT_i^j),$$

$$r_1=\frac{dt}{2dyRe},\quad r_2=\frac{dt}{dy^2Re},$$

Again

$$\frac{\partial T}{\partial t}+\frac{\partial T}{\partial y}=\frac{1}{Pr}\frac{\partial^2 T}{\partial y^2}+\frac{M^2Ec}{Re}u^2$$

$$\frac{T_i^{j+1}-T_i^j}{dt}+\frac{T_{i+1}^{j+1}-T_{i-1}^{j+1}}{2dy}=\frac{1}{Pr}\frac{T_{i+1}^{j+1}-2T_i^{j+1}+T_{i-1}^{j+1}}{dy^2}+\frac{M^2Ec}{Re}(u_i^{j+1})^2$$

$$\left(-\frac{dt}{2dy}-\frac{dt}{Prdy^2}\right)T_{i-1}^{j+1}+\left(1+\frac{2dt}{Prdy^2}\right)T_i^{j+1}\left(\frac{dt}{2dy}-\frac{dt}{Prdy^2}\right)T_{i-1}^{j+1}=T_i^j+\frac{M^2Ecdt}{Re}(u_i^{j+1})^2$$

$$A_2T_{i-1}^{j+1}+B_2T_i^{j+1}+C_2T_{i+1}^{j+1}=D_{2i}^j$$

where

$$A_2=-Re(r_1+\frac{1}{Pr}r_2),\quad B_2=1+2\frac{Re}{Pr}r_2,\quad C_2=Re(r_1-\frac{1}{Pr}r_2),$$

$$D_{2i}^j=T_i^j+\frac{dtM^2Ec}{Re}(u_i^{j+1})^2,$$